The laboratory analysis of Bi II and its application to the Bi-rich HgMn star HR 7775

Dolk, Linus; Litzén, Ulf; Wahlgren, Glenn

Published in:
Astronomy & Astrophysics

DOI:
10.1051/0004-6361:20020573

2002

A&A 388, 692–703 (2002)
DOI: 10.1051/0004-6361:20020573

Astronomy & Astrophysics

The laboratory analysis of Bi II and its application to the Bi-rich HgMn star HR 7775

L. Dolk, U. Litzén, and G. M. Wahlgren

Atomic Astrophysics, Department of Astronomy, Lund University, Box 43, 22100 Lund, Sweden

Received 20 February 2002 / Accepted 11 April 2002

Abstract. The bismuth spectrum emitted from a hollow cathode discharge has been recorded with a Fourier Transform Spectrometer (FTS). Accurate wavelengths have been determined for 104 Bi II lines, and several new energy levels have been found, while the accuracy of previously known Bi II level energies have been improved. The hyperfine structure of all observed Bi II lines has been analyzed, yielding hyperfine constants A and B for 56 Bi II levels. With the aid of the laboratory measurements the optical region spectrum of the HgMn star HR 7775 has been studied for all observable Bi II lines. The wavelengths and hfs constants established from the laboratory work have been combined with theoretical gf values to identify spectral lines and make an abundance estimation of bismuth. It has been established that bismuth is present in HR 7775 at an enhancement level of approximately 5 orders of magnitude relative to the meteoritic abundance, consistent with previous observations in the ultraviolet region of this star. Astrophysical gf values are presented for a number of Bi II lines.

Key words. atomic data – stars: chemically peculiar – stars: individual: HR 7775

1. Introduction

The chemically peculiar (CP) stars of the upper main sequence are recognized by their anomalous abundances for a variety of elements. In a subgroup of CP stars, the HgMn stars, the abundance enhancements of the very heavy elements, Pt, Au, Hg are particularly noticeable, with line depths indicating enhancements of up to 10^6 times the solar value. The two heaviest stable elements, Pb and Bi, have not, however, been observed at a similar enhancement level in HgMn stars, with the exception of bismuth in the HgMn star HR 7775.

The presence of bismuth features in stellar spectra has been reported in a few different type of stars. Guthrie (1972) reported the identification of one Bi I feature in the Ap star 73 Dra. Several strong Bi II features were observed in the ultraviolet region of the HgMn star HR 7775 (Jacobs & Dworetsky 1982), and subsequent synthetic calculations indicated an overabundance of bismuth of approximately 10^6 times compared to the solar system composition. Jacobs & Dworetsky noted that out of a sample of 13 HgMn stars, for which IUE data were analysed, only HR 7775 showed evidence of strong features at the laboratory position of strong Bi II features. The discovery of the strong ultraviolet Bi II lines in HR 7775 by Jacobs & Dworetsky prompted the tentative identification of an optical line at λ4259 as Bi II (Guthrie 1984). Two lines of Bi II were identified on the basis of wavelength coincidence statistics (WCS) from the IUE spectrum of the magnetic Ap star HR 465 (Cowley 1987), and this tentative identification was later substantiated by Fuhrmann (1989). Fuhrmann also reported the possible existence of Bi II features in the Ap star α^2 CVn.

More recently, selected Bi II lines have been studied in the ultraviolet spectrum of the HgMn star χ Lupi (Wahlgren et al. 1994; Leckrone et al. 1998, 1999), with the conclusion that the bismuth abundance is only marginally enhanced in this star. The investigations were made utilizing high-resolution data obtained with the Goddard High Resolution Spectrograph (GHRS) on the Hubble Space Telescope (HST). A recent paper, also utilizing the HST data, considers the bismuth abundance in the two HgMn stars χ Lupi and HR 7775 (Wahlgren et al. 2001). An approximate abundance enhancement of 5 dex for bismuth is noted for HR 7775, while only a moderate abundance enhancement of 0.9 dex is noted for χ Lupi. Thus, the absence of bismuth features in the IUE spectrum of all HgMn stars (except HR 7775) observed by Jacobs & Dworetsky, does not preclude the possibility of a moderate bismuth enhancement in these stars.

It was noted that several unidentified features in the optical region spectrum of HR 7775 coincide with the laboratory positions of Bi II features (Wahlgren et al. 2000). Since several of these features had not been studied for hfs, this served as an incentive to investigate the Bi II spectrum in the laboratory.

Send offprint requests to: L. Dolk,
e-mail: linus.dolk@astro.lu.se

The term system of Bi II presented in Atomic Energy Levels (AEL) (Moore 1958) is based on the laboratory investigation of the Bi II spectrum made by Crawford & McLay (1934) as revised by Murakawa & Suwa (1947). In the paper by Crawford & McLay the spark spectra of Bi II and Bi III were studied and the wavelengths of all observable lines between 1000 Å and 1 μm were measured. It was noted that most of the observed lines had unresolved hyperfine structure (hfs), and hfs intervals were presented for several energy levels.

No general investigation of the Bi II spectrum has been made since the analysis by Crawford & McLay, although accurate wavelength measurements of all observable lines in the 1058–3117 Å region were presented by Wahlgren et al. (2001). These measurements were made at the laboratory resolving power ($R = \lambda/\Delta\lambda = 150\,000$) and wavelengths were reported for all the observed Bi II features, including the hfs components of lines with large enough hfs splittings. There have been several investigations regarding the structure of individual Bi II lines. The hfs of the lowest lying odd and even Bi II configurations have been studied by Cole (1964), Arcimowicz & Dembczynski (1979), Augustyniak & Werel (1984) and Bouazza & Bauche (1988), while the hfs of selected higher excitation energy levels have been presented by Eisele et al. (1968), Stachowska (1987), Stachowska et al. (1987) and Grabowski et al. (1996).

In this paper a thorough laboratory analysis of the Bi II spectrum has been made with a high resolution Fourier Transform Spectrometer (FTS). The specific aim was to improve existing absolute wavelengths and energy levels of Bi II and to analyse the hfs of a large number of Bi II lines for the benefit of astrophysical studies of bismuth in stellar spectra. The laboratory data have been utilized to study several optical region Bi II lines in the spectrum of the HgMn star HR 7775.

2. Experiment

The bismuth spectrum was emitted from a hollow cathode discharge, with the cathode consisting of a water cooled 50 mm long bismuth tube with the inner diameter 5 mm. The discharge was run at 450 mA with neon at 1.5 Torr or argon at 0.5 Torr as carrier gas. The spectra were recorded with a Chelsea Instruments FT500 Fourier transform spectrometer in three overlapping spectral regions, together covering the range 2000–7000 Å. The wavenumber scale was calibrated by means of Ar II lines (Norlén 1973).

Spectral lines from high Bi II levels were enhanced in the Bi:Ne discharge through overpopulation of the high levels by the charge and energy transfer reaction

$$\mathrm{Bi} + \mathrm{Ne}^{+} \rightarrow \mathrm{Bi}^{+*} + \mathrm{Ne} + \Delta E,$$

where the increase of the population has a maximum at ΔE in the range 0.5–1 eV (Johansson & Litzén 1978). This would give an enhancement of lines from Bi II levels in the region 105 000–115 000 cm^{-1} above the Ground state, which is indeed observed. Unexpectedly strong lines are also observed from levels around 125 000–127 000 cm^{-1}, which may be caused by collisions between Ne^{+} ions and bismuth atoms in the metastable $6p^3\ ^2D$ levels 11 419 and 15 437 cm^{-1} above the Ground state. An example of the enhancement is shown in Fig. 1.

3. Analysis of the hyperfine structure

The hfs in all Bi II transitions was analyzed by means of a program in the computer code package IDL (Interactive Data Language, Research Systems, Inc., Boulder), where parameters of a predicted function were fitted to the observed feature. The predicted function, a sum of Gaussians, was based on the following assumptions (as given in Karlsson & Litzén 2001):

1. Each hfs component has a Doppler profile.
2. The hyperfine level splitting depends on the magnetic dipole and the electric quadrupole interaction according to

$$\Delta E = \frac{1}{2}AC + \frac{B}{4}\frac{\frac{3}{2}C(C+1) - 2I(I+1)J(J+1)}{I(2I-1)J(2J-1)}$$

   where $C = F(F+1) - I(I+1) - J(J+1)$.
3. The intensities of the individual components are distributed according to the corresponding line strength relations in a multiplet at pure LS coupling.

The free parameters in the analysis were the centre-of-gravity wavenumber of the hfs-pattern, the intensity of the strongest component, the Doppler width of the components and the hfs constants A and B for the upper and the lower level.

In the analysis transitions where one of the levels had $J = 0$ and the other level $J = 1$ were first studied. This means that the feature will depend on only one A and one B parameter and only consist of three well resolved components. The fitting routine is then rather insensitive to the starting values of the parameters. Then successively more complicated structures were analyzed, where the A and B from a previous fit could be fixed or used as starting values for one of the involved levels. In the cases where the A and B parameters of a level were fixed for the analysis of a line, a second run was made allowing the values to be changed. This was done in order to reduce a propagation of errors in the A and B values.

4. The Bi II spectral lines and energy levels

All the Bi II spectral lines observed and analyzed in the present work are shown in Table 1. The wavenumbers in column three represent the centres-of-gravity of the hfs patterns, derived as described in the previous section. The corresponding wavelengths are shown in column two, where the air wavelengths above 2000 Å were derived by means of Edlén's dispersion formula (Edlén 1966). The uncertainty of the wavenumbers is estimated as varying

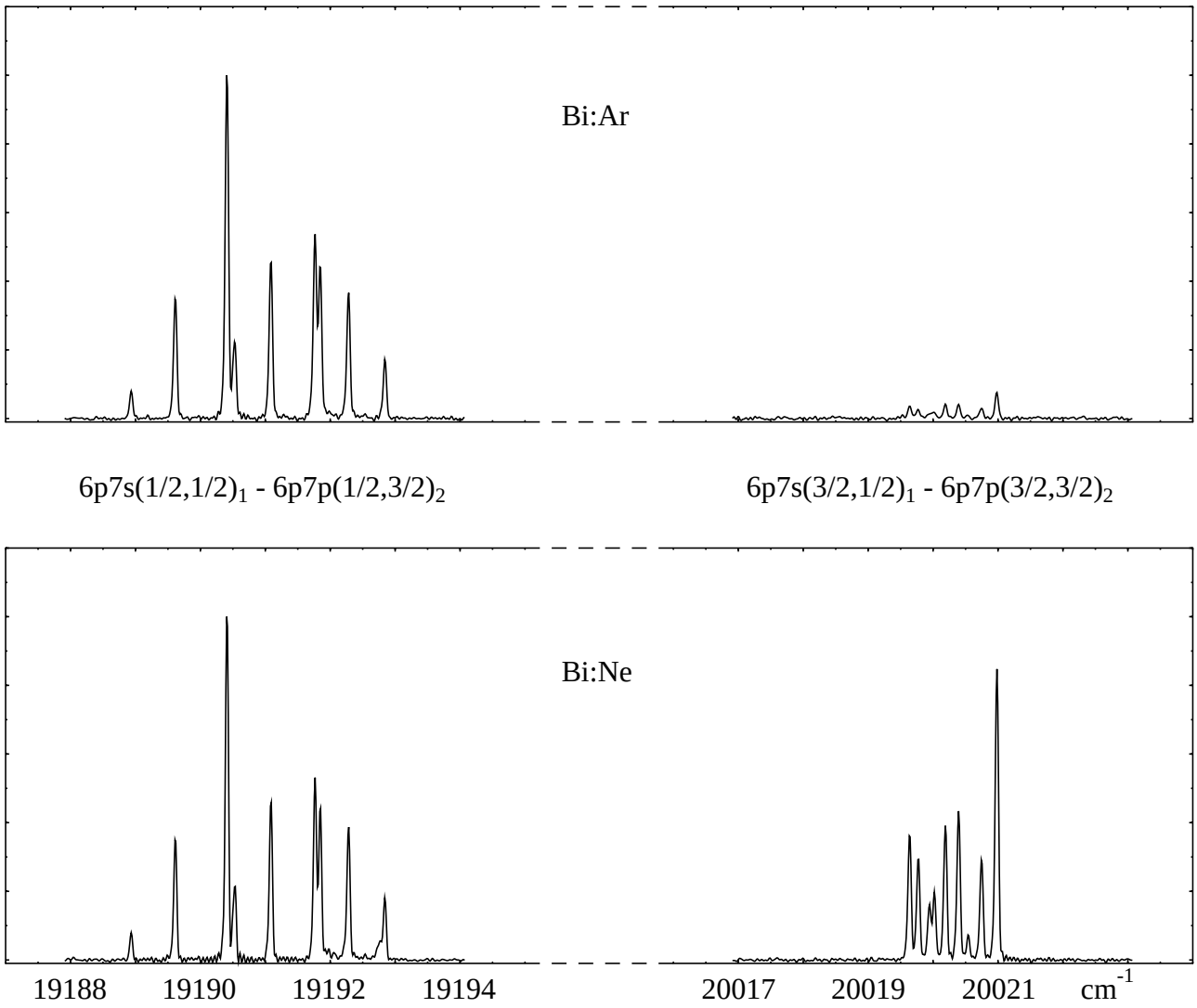

Fig. 1. An example of the enhancement of a Bi II line in the Bi:Ne discharge through overpopulation of a high level caused by collisions between Ne^+ ions and bismuth atoms.

from 0.003 cm^{-1} for strong lines with well resolved hfs patterns to 0.05 cm^{-1} for weak lines with complex hfs. This corresponds to 0.001–0.02 Å at 6000 Å and 0.0001–0.002 Å at 2000 Å. The intensity noted in the first column represents the signal-to-noise ratio (SNR) of the strongest peak of the observed hfs pattern, and is thus strongly affected by the charge and energy transfer reactions in the light source. The fourth column shows the difference between the observed wavenumber of a line and the wavenumber derived from the improved energy level values (see below). This difference is only shown for lines where more than one line was used for establishing the upper energy level. The last column of the table contains the designations of the combining levels as discussed below.

Besides the lines observed in the present work the table also contains three lines below 2000 Å, viz. the λ1902 line from Wahlgren et al. (1994) and λ1436 and λ1791 from Wahlgren et al. (2001). These lines were used for providing accurate connections between the Bi II Ground state and the excited configurations.

The energy level values derived from the lines of Table 1 are shown in Tables 2 and 3, and an overview of the energy level system can be seen in Fig. 2. The level values were optimized by means of the computer code ELCALC (Radziemski et al. 1972). The uncertainty of the relative energy level values of the excited configurations is estimated as varying from 0.002 cm^{-1} for levels connected by several lines to 0.05 cm^{-1} for levels established by only one, weak line. The uncertainty of the values of the absolute energy levels relative to the ground term depends on the accuracy of the line at 1436 Å, stated in Wahlgren et al. (2001) as 0.0010 Å or 0.05 cm^{-1}.

Tables 2 and 3 also contain the hyperfine constants A and B derived from the analysis of the hfs patterns as described in a previous section. For levels involved in more than one transition the A and B values are averaged from the different transitions, weighted according to the SNR of the observed feature. The uncertainties shown in the tables represent estimated fitting errors of the derived hfs constants. These errors were determined

Table 1. Observed Bi II lines.

Int[a]	λ[b] (Å)	σ (cm^{-1})	$o-c$	Combination		
24	6809.1955	14681.971	0.000	6p7s $(1/2,1/2)_1$	-	6p7p $(1/2,1/2)_1$
26	6600.3388	15146.554	−0.001	6p7s $(1/2,1/2)_0$	-	6p7p $(1/2,1/2)_1$
5	6059.1102	16499.505		6p7s $(3/2,1/2)_2$	-	6p7p $(3/2,1/2)_1$
58	5719.1384	17480.302	0.000	6p7s $(1/2,1/2)_1$	-	6p7p $(1/2,1/2)_0$
6	5655.1659	17678.041	−0.003	6p7s $(3/2,1/2)_2$	-	6p5f $(1/2,5/2)_2$
3	5501.2997	18172.474	0.002	6p7d $(1/2,3/2)_1$	-	6p5f $(3/2,5/2)_2$
6	5490.3705	18208.648	0.000	$6s6p^3\ ^3D_1$	-	6p7p $(3/2,3/2)_0$
4	5397.8894	18520.610	0.001	6p7s $(3/2,1/2)_1$	-	6p7p $(3/2,3/2)_1$
8	5361.9475	18644.755	−0.001	6p6d $(3/2,5/2)_3$	-	6p5f $(3/2,5/2)_4$
31	5270.5120	18968.210	0.000	6p7s $(1/2,1/2)_1$	-	6p7p $(1/2,3/2)_1$
4	5245.8158	19057.507	−0.003	6p7d $(1/2,3/2)_1$	-	6p5f $(3/2,7/2)_2$
191	5209.3246	19191.003	0.000	6p7s $(1/2,1/2)_1$	-	6p7p $(1/2,3/2)_2$
2	5201.5800	19219.576	−0.003	6p7p $(1/2,3/2)_2$	-	6p6d $(3/2,5/2)_3$
2	5201.5232	19219.786	0.000	6p7s $(3/2,1/2)_1$	-	6p8p $(1/2,3/2)_1$
121	5144.4921	19432.851	0.057	6p7s $(1/2,1/2)_0$	-	6p7p $(1/2,3/2)_1$
57	5124.3561	19509.211	0.001	6p7s $(3/2,1/2)_2$	-	6p7p $(3/2,3/2)_3$
10	5091.5684	19634.841	0.000	6p7s $(3/2,1/2)_2$	-	6p7p $(3/2,3/2)_1$
157	4993.5338	20020.313	0.001	6p7s $(3/2,1/2)_1$	-	6p7p $(3/2,3/2)_2$
8	4969.5134	20117.081	0.005	6p7s $(3/2,1/2)_2$	-	6p8p $(1/2,3/2)_2$
5	4876.6967	20499.958	0.001	6p5f $(1/2,5/2)_2$	-	6p7d $(3/2,3/2)_3$
7	4749.7270	21047.955	−0.001	6p7p $(1/2,1/2)_0$	-	6p7d $(1/2,3/2)_1$
74	4730.2672	21134.543	−0.001	6p7s $(3/2,1/2)_2$	-	6p7p $(3/2,3/2)_2$
72	4705.2854	21246.751		6p7p $(1/2,1/2)_1$	-	6p7d $(1/2,3/2)_2$
7	4572.4659	21863.910	−0.002	6p7p $(3/2,1/2)_2$	-	6p7d $(3/2,3/2)_3$
2	4493.9702	22245.798	0.004	6p6d $(3/2,3/2)_3$	-	6p8f $(1/2,7/2)_4$
5	4466.5746	22382.240	−0.001	6p6d $(3/2,3/2)_3$	-	6p5f $(3/2,5/2)_3$
2	4436.6820	22533.040	−0.005	6p6d $(3/2,3/2)_3$	-	6p5f $(3/2,7/2)_4$
188	4391.4358	22765.200	0.000	6p7s $(3/2,1/2)_1$	-	6p7p $(3/2,3/2)_0$
8	4340.4737	23032.485	0.004	6p6d $(1/2,5/2)_3$	-	6p5f $(1/2,7/2)_3$
3	4339.8307	23035.897	−0.003	6p6d $(1/2,5/2)_2$	-	6p7p $(3/2,1/2)_2$
2	4336.4052	23054.094	0.016	6p6d $(3/2,3/2)_2$	-	6p5f $(3/2,5/2)_3$
64	4301.6974	23240.100	0.000	6p6d $(1/2,5/2)_2$	-	6p5f $(1/2,7/2)_3$
17	4272.0440	23401.413	0.000	6p6d $(1/2,5/2)_2$	-	6p5f $(1/2,5/2)_3$
124	4259.4126	23470.809		6p6d $(1/2,5/2)_3$	-	6p5f $(1/2,7/2)_4$
50	4227.0843	23650.308	0.000	6p6d $(3/2,3/2)_3$	-	6p5f $(3/2,5/2)_4$
54	4204.7421	23775.973	−0.001	6p6d $(3/2,3/2)_2$	-	6p5f $(3/2,7/2)_3$
6	4171.1345	23967.537	0.000	6p6d $(3/2,3/2)_2$	-	6p5f $(3/2,5/2)_2$
3	4097.2286	24399.855	0.000	6p6d $(1/2,5/2)_2$	-	6p5f $(1/2,5/2)_2$
99	4079.0719	24508.461	0.000	6p6d $(1/2,3/2)_1$	-	6p7p $(3/2,1/2)_2$
2	4022.5909	24852.576	0.001	6p6d $(3/2,3/2)_2$	-	6p5f $(3/2,7/2)_2$
6	4005.4745	24958.775	0.000	6p8s $(1/2,1/2)_1$	-	6p5f $(3/2,5/2)_2$
6	3905.2689	25599.180	0.000	6p8s $(1/2,1/2)_0$	-	6p5f $(3/2,5/2)_1$
41	3874.2291	25804.272	−0.002	6p6d $(3/2,3/2)_1$	-	6p5f $(3/2,5/2)_2$
55	3871.2853	25823.894	0.000	6p7p $(1/2,3/2)_2$	-	6p9s $(1/2,1/2)_1$
70	3864.0245	25872.418	0.002	6p6d $(1/2,3/2)_1$	-	6p5f $(1/2,5/2)_2$
10	3845.8928	25994.392	0.001	6p6d $(1/2,3/2)_2$	-	6p7p $(3/2,1/2)_2$
34	3843.2278	26012.417	0.001	6p7p $(1/2,3/2)_1$	-	6p9s $(1/2,1/2)_0$
10	3838.1712	26046.686	−0.001	6p7p $(1/2,3/2)_1$	-	6p9s $(1/2,1/2)_1$
35	3827.0261	26122.538	0.000	6p6d $(3/2,5/2)_2$	-	6p8f $(1/2,5/2)_3$
33	3815.9162	26198.591	0.000	6p6d $(1/2,3/2)_2$	-	6p5f $(1/2,7/2)_3$
15	3812.5219[c]	26221.915		6p6d $(1/2,5/2)_4$	-	6p5f $(1/2,7/29_5$
17	3811.1984	26231.021	0.000	6p6d $(1/2,5/2)_2$	-	6p7p $(3/2,3/2)_3$
203	3792.5636	26359.904	0.000	6p6d $(1/2,3/2)_2$	-	6p5f $(1/2,5/2)_3$
32	3790.4766	26374.417	−0.001	6p6d $(3/2,5/2)_2$	-	6p5f $(3/2,5/2)_3$
22	3762.9021	26567.684	0.000	6p6d $(3/2,3/2)_1$	-	6p5f $(3/2,5/2)_1$
17	3745.7530	26689.315	0.003	6p6d $(3/2,3/2)_1$	-	6p5f $(3/2,7/2)_2$
32	3719.1568	26880.169	0.000	6p6d $(3/2,3/2)_0$	-	6p5f $(3/2,5/2)_1$
25	3689.4887	27096.314	0.000	6p6d $(3/2,5/2)_2$	-	6p5f $(3/2,7/2)_3$
8	3654.1507	27358.346	0.000	6p6d $(1/2,3/2)_2$	-	6p5f $(1/2,5/2)_2$
18	3630.7598	27534.595	0.000	6p7p $(1/2,1/2)_0$	-	6p9s $(1/2,1/2)_1$

Table 1. continued.

Int[a]	λ^b (Å)	σ (cm^{-1})	$o-c$	Combination		
4	3615.7701	27648.741	0.005	6p6d $(1/2,5/2)_3$	-	6p7p $(3/2,3/2)_2$
8	3523.0817	28376.128	0.000	6p7p $(1/2,3/2)_1$	-	6p8d $(1/2,5/2)_2$
23	3515.7776	28435.078		6p7p $(1/2,3/2)_2$	-	6p8d $(1/2,5/2)_3$
47	3430.6054	29141.019	−0.001	6s6p^3 ^{5}S$_2$	-	6p5f $(1/2,7/2)_3$
10	3425.2072	29186.945	0.002	6s6p^3 ^{3}D$_3$	-	6p8f $(1/2,7/2)_4$
5	3409.2689	29323.389	−0.001	6s6p^3 ^{3}D$_3$	-	6p5f $(3/2,5/2)_3$
12	3408.6264	29328.916	0.000	6p6d $(1/2,3/2)_1$	-	6p7p $(3/2,3/2)_2$
51	3391.8248	29474.194	0.000	6s6p^3 ^{3}D$_3$	-	6p5f $(3/2,7/2)_4$
13	3327.3521	30045.285	−0.001	6s6p^3 ^{3}D$_3$	-	6p5f $(3/2,7/2)_3$
12	3309.9520	30203.225	−0.001	6s6p^3 ^{3}D$_2$	-	6p8f $(1/2,5/2)_3$
15	3299.5266	30298.654	−0.001	6p7p $(1/2,1/2)_1$	-	6p9s $(1/2,1/2)_0$
17	3295.7984	30332.926	0.000	6p7p $(1/2,1/2)_1$	-	6p9s $(1/2,1/2)_1$
36	3282.5759	30455.106	0.000	6s6p^3 ^{3}D$_2$	-	6p5f $(3/2,5/2)_3$
8	3186.9830	31368.568	0.003	6s6p^3 ^{3}D$_2$	-	6p5f $(3/2,5/2)_2$
25	3116.9054	32073.803	−0.001	6p6d $(1/2,3/2)_1$	-	6p7p $(3/2,3/2)_0$
3	3111.2661	32131.936	−0.005	6s6p^3 ^{5}S$_2$	-	6p7p $(3/2,3/2)_3$
5	3060.7375	32662.369	0.002	6p7p $(1/2,1/2)_1$	-	6p8d $(1/2,5/2)_2$
2	2968.3174	33679.285	−0.020	6p6d $(1/2,5/2)_3$	-	6p6f $(1/2,5/2)_3$
25	2950.4167	33883.615		6p6d $(1/2,5/2)_3$	-	6p6f $(1/2,7/2)_4$
12	2936.7450	34041.349	0.001	6p6d $(1/2,5/2)_2$	-	6p6f $(1/2,7/2)_3$
31	2805.2213	35637.311	−0.001	6p6d $(1/2,3/2)_1$	-	6p6f $(1/2,5/2)_2$
12	2803.4556	35659.756	−0.001	6p^2 ^{1}D$_2$	-	6p7s $(1/2,1/2)_1$
2	2745.4201	36413.528	−0.002	6p7s $(3/2,1/2)_1$	-	6p5f $(3/2,5/2)_2$
100	2713.2377	36845.415	0.000	6p6d $(1/2,3/2)_2$	-	6p6f $(1/2,5/2)_3$
2	2701.9136	36999.831	−0.008	6p6d $(1/2,3/2)_2$	-	6p6f $(1/2,7/2)_3$
7	2692.9308	37123.244	0.002	6p6d $(1/2,3/2)_2$	-	6p6f $(1/2,5/2)_2$
5	2680.2723	37298.561	−0.007	6p7s $(3/2,1/2)_1$	-	6p5f $(3/2,7/2)_2$
7	2630.9622	37997.579	0.000	6p7p $(1/2,1/2)_1$	-	6p9d $(1/2,3/2)_2$
11	2544.4103	39290.041	−0.003	6p7s $(1/2,1/2)_1$	-	6p8p $(1/2,3/2)_2$
4	2530.4375	39506.982	−0.004	6p7s $(1/2,1/2)_1$	-	6p8p $(1/2,3/2)_1$
2	2514.6745	39754.610		6p7p $(1/2,3/2)_2$	-	6p7d $(3/2,5/2)_3$
5	2512.5739	39787.844	0.000	6s6p^3 ^{5}S$_2$	-	6p6f $(1/2,5/2)_3$
37	2502.8591	39942.269	0.001	6s6p^3 ^{5}S$_2$	-	6p6f $(1/2,7/2)_3$
6	2501.0242	39971.571		6p7s $(1/2,1/2)_0$	-	6p8p $(1/2,3/2)_1$
4	2495.1499	40065.670	−0.001	6s6p^3 ^{5}S$_2$	-	6p6f $(1/2,5/2)_2$
13	2480.1781	40307.512	0.000	6p7s $(1/2,1/2)_1$	-	6p7p $(3/2,3/2)_2$
6	2418.7166	41331.683		6p7p $(1/2,1/2)_1$	-	6p10d $(1/2,3/2)_2$
54	2368.3838	42209.992	−0.002	6p^2 ^{1}D$_2$	-	6s6p^3 ^{5}S$_2$
4	2325.2984	42992.034	−0.014	6p6d $(1/2,5/2)_3$	-	6p8f $(1/2,7/2)_4$
3	2251.7291	44396.556	−0.006	6p6d $(1/2,5/2)_3$	-	6p5f $(3/2,5/2)_4$
18	2214.0307	45152.425	0.002	6p^2 ^{1}D$_2$	-	6p6d $(1/2,3/2)_2$
37	2186.9297	45711.907	0.000	6p^2 ^{1}S$_0$	-	6p7s $(3/2,1/2)_1$
5	2143.4827	46638.356	0.003	6p^2 ^{1}D$_2$	-	6p6d $(1/2,3/2)_1$
200	1902.3422[d]	52566.777	0.000	6p^2 ^{3}P$_2$	-	6p7s $(1/2,1/2)_1$
100	1791.842[e]	55808.49	0.000	6p^2 ^{3}P$_1$	-	6p7s $(1/2,1/2)_0$
500	1436.8130[e]	69598.475	0.000	6p^2 ^{3}P$_0$	-	6p7s $(1/2,1/2)_1$

[a] Signal-to-noise ratio of the strongest component. [b] Centre of gravity air wavelength above 2000 Å and vacuum wavelength below 2000 Å. [c] Tentative identifiction, the energy levels in the transition can not be substantiated from other lines. [d] Measured by Wahlgren et al. (1994). [e] Measured by Wahlgren et al. (2001).

by comparing the hfs constants derived from all transitions involving a specific level. The criteria for deriving errors included considerations of line intensities, number of lines involving the levels, as well as line blending issues. A statistical approach was neglected since only one or a few lines were involved in the determination of the hfs constants of most levels, which could lead to erratic results in the uncertainty estimates. In cases where only one transition was observed, the uncertainty was estimated from the uncertainties of constants derived from lines with similar

Table 2. Bi II even levels.

Designation	J	Energy (cm^{-1})	Eigenvector comp.[a] (%)		Hyperfine constants[b] A (mK)	B (mK)	Other exp.[b] A (mK)	B (mK)	Ref.[c]
$6p^2\ ^3P$	0	0.000[d]	83 ^3P	17 ^1S					
$6p^2\ ^3P$	1	13325.401[d]	100 ^3P				−82.9 (1)	−16.5 (10)	[1]
							−82.5 (7)	−15.5 (35)	[2]
							−82.85	−15.7	[3]
$6p^2\ ^3P$	2	17031.698	52 ^3P	48 ^1D	112.6 (3)	−10 (5)	112.6 (1)	−8 (1)	[1]
							115.1 (28)	−72 (161)	[2]
$6p^2\ ^1D$	2	33938.718	52 ^1D	48 ^3P	27.4 (1)	−24 (2)	27.4 (2)	−29 (3)	[1]
							27.5 (7)	−12 (16)	[2]
							27.18 (11)	−8.3 (16)	[4]
$6p^2\ ^1S$	0	44173.768	82 ^1S	17 ^3P					
6p7p (1/2,1/2)	1	84280.446	100 (1/2,1/2)		269.25 (5)	1 (2)	270.7 (6)	−0.6 (18)	[5]
6p7p (1/2,1/2)	0	87078.777	98 (1/2,1/2)						
6p7p (1/2,3/2)	1	88566.685	100 (1/2,3/2)		−102.10 (5)	−1 (1)	−102.5 (3)	−0.2 (3)	[5]
6p7p (1/2,3/2)	2	88789.478	99 (1/2,3/2)		123.35 (10)	−12 (2)	123.6 (3)	−6.2 (21)	[5]
6p7p (3/2,1/2)	2	105085.532	50 (3/2,1/2)	47 5f(1/2,5/2)	−13.6 (3)	−20 (8)			
6p7p (3/2,1/2)	1	105270.947	85 (3/2,1/2)	13 (3/2,3/2)	13.3 (8)	−10 (10)	17.4 (10)	−2.1 (21)	[5]
6p5f (1/2,7/2)	3	105289.732	82 (1/2,7/2)	13 7p(3/2,3/2)	−28.8 (2)	−8 (4)			
6p5f (1/2,5/2)	3	105451.045	95 (1/2,5/2)		56.9 (4)	5 (5)			
6p5f (1/2,7/2)	4	105728.060	100 (1/2,7/2)		59.1 (3)	−6 (5)			
6p5f (1/2,5/2)	2	106449.487	51 (1/2,5/2)	41 7p(3/2,1/2)	−23.25 (20)	−13 (5)	−21.0 (8)	−12.9 (83)	[5]
6p7p (3/2,3/2)	3	108280.653	86 (3/2,3/2)	13 5f(1/2,7/2)	10.4 (2)	−40 (10)	11.3 (4)	−16.1 (21)	[5]
6p7p (3/2,3/2)	1	108406.284	76 (3/2,3/2)	14 (3/2,1/2)	−13.7 (4)	8 (5)			
6p8p (1/2,3/2)	2	108888.519	73 (1/2,3/2)	26 7p(3/2,3/2)	101.4 (4)	6 (5)	101.8 (12)	1.1 (35)	[5]
6p8p (1/2,3/2)	1	109105.461	92 (1/2,3/2)		−69.8 (3)	−7 (5)			
6p7p (3/2,3/2)	2	109905.987	69 (3/2,3/2)	22 8p(1/2,3/2)	37.05 (10)	−8 (3)	37.2 (6)	−12.7 (26)	[5]
6p7p (3/2,3/2)	0	112650.875	89 (3/2,3/2)	5 8p(1/2,1/2)					
6p6f (1/2,5/2)	3	115936.556	100 (1/2,5/2)		78.95 (20)	−5 (10)			
6p6f (1/2,7/2)	3	116090.980	99 (1/2,7/2)		−57.75 (10)	25 (3)			
6p6f (1/2,7/2)	4	116140.866	100 (1/2,7/2)		59.5 (5)	40 (20)			
6p6f (1/2,5/2)	2	116214.383	99 (1/2,5/2)		−78.0 (2)	−2 (8)			
6p8f (1/2,5/2)	3	125133.866	72 (1/2,5/2)	16 (1/2,7/2)	22.5 (2)	−9 (5)			
6p8f (1/2,7/2)	4	125249.299	88 (1/2,7/2)	12 5f(3/2,7/2)	51.6 (8)	–			
6p5f (3/2,5/2)	3	125385.746	82 (3/2,5/2)	8 8f(1/2,5/2)	19.2 (3)	7 (6)	15 (6)	-	[6]
6p5f (3/2,7/2)	4	125536.550	72 (3/2,7/2)	18 (3/2,5/2)	11.2 (3)	0 (10)	5 (10)	-	[6]
6p5f (3/2,7/2)	3	126107.642	84 (3/2,7/2)	9 (3/2,5/2)	−2.5 (5)	27 (5)	−11 (3)	-	[6]
6p5f (3/2,7/2)	5	126266.[e]	100 (3/2,7/2)		−34 (2)	100 (50)			
6p5f (3/2,5/2)	2	126299.205	91 (3/2,5/2)		8.2 (3)	23 (7)	11	-	[6]
6p5f (3/2,5/2)	4	126653.813	81 (3/2,5/2)	16 (3/2,7/2)	12.60 (15)	−36 (5)			
6p5f (3/2,5/2)	1	127062.615	98 (3/2,5/2)		−18.55 (15)	−4 (2)			
6p5f (3/2,7/2)	2	127184.243	97 (3/2,7/2)		−15.5 (3)	−18 (5)			

[a] The two largest eigenvector components. The second component is shown only in cases where the largest components is smaller than 90%. Configuration is shown for the second component when it is not the same as for the first component.
[b] Numbers in parenthesis represents an estimated fitting error for the last digit(s).
[c] References to previous A and B determinations: [1] Bouazza & Bauche (1988); [2] Cole (1964); [3] George et al. (1985); [4] Arcimowicz & Dembczynski (1979); [5] Grabowski et al. (1996); [6] Stachowska et al. (1987).
[d] The connection between the two lowest levels of the $6p^2$ ground configuration and the excited configurations is established by the lines at 1436 Å and 1791 Å reported by Wahlgren et al. (2001).
[e] Level value from the parametric fit. The hfs constants were derived from a line tentatively identified as the combination with $6p6d(3/2,5/2)_4$, but the latter level is not connected to the rest of the system. The uncertainty of the level is estimated to ± 400 cm^{-1}, based on comparisons to Cowan calculations of other levels.

SNR and complexity. In the last columns of Tables 2 and 3 hfs constants from previous measurements are presented with their uncertainties and references.

All levels presented in AEL III (Moore 1958) have been confirmed by our data, except those at 107 976, 115 990 and 117 004 cm^{-1}. These levels were observed by Crawford & McLay (1934), but transitions involving these levels can not be found in our spectra. The Cowan calculations in this paper predict energy levels with corresponding J values near 107 976 and 117 004 cm^{-1}, but fail to predict a level near 115 990 cm^{-1}. In the paper by Crawford & McLay this level is listed as a tentative

Table 3. Bi II odd levels.

Designation	J	Energy (cm^{-1})	Eigenvector comp.[a] (%)		Hyperfine constants[b] A (mK)	B (mK)	Other exp.[b] A (mK)	B (mK)	Ref.[c]
6p7s (1/2,1/2)	0	69133.891	100 (1/2,1/2)						
6p7s (1/2,1/2)	1	69598.475	98 (1/2,1/2)		390.7 (1)	3 (1)	391.1 (1)	2.8 (6)	[1]
							392.1 (7)	0.6 (11)	[2]
							390.70	3.3	[3]
							390.74 (5)	2.3 (3)	[4]
6s6p^3 ^{5}S	2	76148.712	55 ^{5}S	18 ^{3}P	401.30 (5)	−12 (8)	401.35 (11)	−9.4 (16)	[5]
6p6d (1/2,3/2)	2	79091.141	97 (1/2,3/2)		119.5 (5)	0 (5)			
6p6d (1/2,3/2)	1	80577.071	73 (1/2,3/2)	13 p^3 ^{3}D	−174.1 (2)	−5 (2)			
6p6d (1/2,5/2)	2	82049.632	71 (1/2,5/2)	26 p^3 ^{5}S	90.75 (20)	10 (2)			
6p6d (1/2,5/2)	3	82257.251	94 (1/2,5/2)		84.0 (2)	0 (4)			
6p7s (3/2,1/2)	2	88771.443	99 (3/2,1/2)		106.0 (2)	−38 (3)	106.0 (1)	−38 (1)	[1]
							107.8 (3)	−34.5 (29)	[2]
6p7s (3/2,1/2)	1	89885.675	84 (3/2,1/2)	6 6d(3/2,5/2)	−60.6 (1)	−22 (2)	−60.6 (1)	−21 (1)	[1]
							−61.4 (8)	−25.9 (30)	[2]
							−60.71 (50)	−21.5 (5)	[4]
6s6p^3 ^{3}D	1	94442.227	44 ^{3}D	22 6d(1/2,3/2)	−307.9 (5)	−23 (10)	−305 (1)	−50 (4)	[6]
6s6p^3 ^{3}D	2	94930.640	48 ^{3}D	31 6d(3/2,3/2)	76.5 (5)	−15 (10)	70 (10)	−36 (1)	[6]
6s6p^3 ^{3}D	3	96062.356	50 ^{3}D	31 6d(3/2,5/2)	201.3 (2)	−9 (5)	196 (8)		[6]
6p6d (3/2,5/2)	2	99011.328	55 (3/2,5/2)	19 (3/2,3/2)	108.9 (4)	−12 (6)			
6p6d (3/2,5/2)	4	99405.[d]	100 (3/2,5/2)		9 (2)	11 (20)			
6p6d (3/2,3/2)	0	100182.446	72 (3/2,3/2)	18 p^3 ^{3}P					
6p6d (3/2,3/2)	1	100494.931	64 (3/2,3/2)	12 6d(3/2,5/2)	108.4 (3)	11 (4)			
6p8s (1/2,1/2)	1	101340.430	86 (1/2,1/2)	11 6d(3/2,3/2)	279.8 (8)	6 (10)			
6p8s (1/2,1/2)	0	101463.435	90 (1/2,1/2)	10 6d(3/2,3/2)					
6p6d (3/2,3/2)	2	102331.668	38 (3/2,5/2)	34 (3/2,3/2)	100.3 (5)	8 (5)			
6p6d (3/2,3/2)	3	103003.505	59 (3/2,3/2)	28 7d(1/2,5/2)	79.1 (3)	−30 (5)			
6p7d (1/2,3/2)	2	105527.197	95 (1/2,3/2)		116.2 (2)	5 (3)			
6p6d (3/2,5/2)	1	106611.224[e]	64 (3/2,5/2)	13 7d(1/2,3/2)					
6p6d (3/2,5/2)	3	108009.057	41 (3/2,5/2)	36 7d(1/2,5/2)	56.3 (4)	−25 (10)			
6p7d (1/2,3/2)	1	108126.733	75 (1/2,3/2)	8 6d(3/2,5/2)	−20.9 (7)	0 (10)			
6p7d (1/2,5/2)	2	109158.128[e]	34 (1/2,5/2)	31 p^3 ^{3}D			170 (6)	10 (10)	[6]
6p9s (1/2,1/2)	0	114579.101	87 (1/2,1/2)	11 p^3 ^{3}P					
6p9s (1/2,1/2)	1	114613.372	76 (1/2,1/2)	9 p^3 ^{3}P	218.15 (10)	−18 (1)			
6p8d (1/2,5/2)	2	116942.813	49 (1/2,5/2)	40 (1/2,3/2)	35.65 (20)	5 (3)			
6p8d (1/2,5/2)	3	117224.556	96 (1/2,5/2)		71.3 (3)	5 (10)			
6p9d (1/2,3/2)	2	122278.025	89 (1/2,3/2)		117.3 (5)	−30 (10)			
6p10d (1/2,3/2)	2	125612.129	90 (1/2,3/2)		100.0 (5)	−10 (5)			
6p7d (3/2,3/2)	3	126949.444	72 (3/2,3/2)	26 (3/2,5/2)	23.6 (3)	−21 (6)			
6p7d (3/2,5/2)	3	128544.088	71 (3/2,5/2)	26 (3/2,3/2)	−31 (1)				

[a] The two largest eigenvector components. The second component is shown only in cases where the largest components is smaller than 90%. Configuration is shown for the second component when it is not the same as for the first component.
[b] Numbers in parenthesis represents an estimated fitting error for the last digit(s).
[c] References to previous A and B determinations: [1] Bouazza & Bauche (1988); [2] Grabowski et al. (1996); [3] George et al. (1985); [4] Eisele et al. (1968); [5] Arcimowicz & Dembczynski (1979); [6] Stachowska et al. (1987).
[d] Level value from the parametric fit. The hfs constants were derived from a line tentatively identified as the combination with 6p5f(3/2,7/2)$_5$, but the latter level is not connected to the rest of the system. The uncertainty of the level is estimated to ±400 cm^{-1}, based on comparisons to Cowan calculations of other levels.
[e] Level value derived from VUV lines reported in Wahlgren et al. (2001). No combinations observed in the present work.

identification from one weak spectral feature. Two other AEL levels, the odd levels at 106 611 and 109 158 cm^{-1}, have not been confirmed in the present work, but as they are confirmed by combinations reported by Wahlgren et al. (2001), they are included in Table 3. The J values of two levels (105 270, 106 449) have been changed. Five levels established by Stachowska et al. (1987) have also been confirmed, but the J of the level at 125 536 cm^{-1} has been changed from 2 to 4. The changes of J values are based on the hfs analysis and the theoretical interpretation of the level structure.

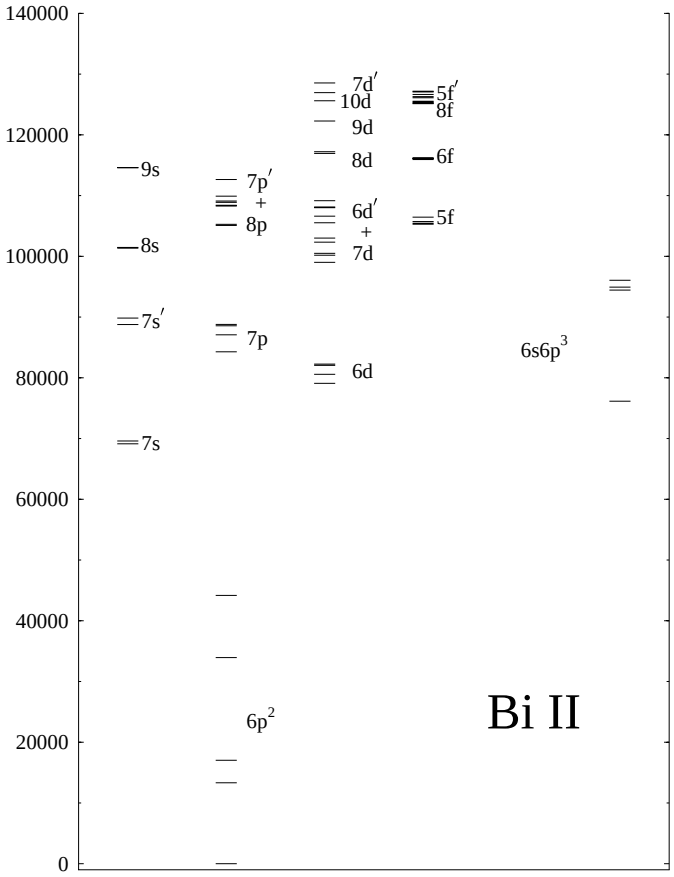

Fig. 2. An overview of the energy level system of Bi II.

Identification of a number of previously unidentified lines have enabled the establishment of 17 new levels. Some of the high levels are derived from only one line, but in these cases the identity of the lower level can be unambiguously established by means of the hyperfine constants derived from the analysis of the hfs pattern.

Two new levels, the $J = 4$ level of 6p6d and the $J = 5$ level of 6p5f, have not been connected to the rest of the system by any observed line. A tentative identification of a line representing the transition between the two levels is given in Table 1. This identification is based on the position of the line predicted by the theoretical calculations described below, and on the observed hfs pattern, consistent with the pattern expected for a $J = 4 \Leftrightarrow 5$ transition. In fact, it is the only line with hyperfine structure observed in our work that can not be identified in any other way. The connection of the two levels to the rest of the system is difficult, as they are the highest J levels of each configuration, and the lower level, $J = 4$ of 6p6d, is metastable.

5. A theoretical study of the Bi II energy level structure

The ground configuration of Bi II is $6p^2$ and the excited configurations belong to the 6pnl system (see Fig. 2). Also, the inner-shell excited configuration $6s6p^3$ is situated below the first ionization limit. As expected for the heaviest elements in the periodic table, the level structure of Bi II can not be well described by the LS coupling approximation. The magnetic spin-orbit interaction is large, giving a fine structure splitting of the 6p ^{2}P parent term of 20 788 cm^{-1}. This could be compared to the corresponding parent splitting of the homologous N II system, amounting to 174 cm^{-1}. This means that the structure can be represented by the jj coupling approximation, and the level designations used in this work are based on this coupling. The designations have the form $6pnl(j_{6p},j_{nl})_J$.

The large parent splitting gives rise to a particular complication in the interpretation of the structure, as each 6pnl configuration is split in two groups, separated by a distance equal to the parent splitting. As this splitting is of the same magnitude or larger than the distance between the average energies of adjacent configurations, the configurations will overlap, and will in certain regions be strongly mixed. This can be seen in Fig. 2, where the lower and the upper group of levels in each configuration are given the labels nl and nl'. This corresponds to $j_{6p} = 1/2$ and $j_{6p} = 3/2$ in the jj notation.

In the present work the observed structure has been interpreted by the set of computer programs known as the Cowan code (Cowan 1981). An ab inito calculation with Hartree-Fock wave functions was followed by a parametric study, where significant energy parameters were fitted to the observed levels. All electrostatic energy integrals were scaled to 80% of the Hartree-Fock values in the ab inito calculation, as this is known to improve the agreement with the observed structure (Cowan 1981). This scaling was maintained for the parameters that were fixed during the parametric fit. The major eigenvector components of the observed levels, derived from the parametric calculations, are shown in Tables 2 and 3.

5.1. The even configurations

The calculations comprised the configurations $6p^2$, 6p7p, 6p8p, and 6p5f–6p8f. As the purity of the levels of the $6p^2$ ground configuration is the same in LS and jj coupling, we have chosen to use the more familiar LS designation for these levels. The strongest configuration mixings, caused by complete overlap, appear between 6p7p and 6p8p and between 6p7p and 6p5f. The Hartree-Fock and the fitted parameter values are shown in Table 4. All parameters of 6p7f were fixed at 100% or 80% of the Hartree-Fock values, as no levels of this configuration were observed. This is probably due to the fact that these levels are predicted to appear in a region where no enhancement due to charge and energy exchange in the light source is expected.

All configuration interaction parameters representing interactions other than these mentioned above are not shown in the table, since they are considered to be of peripheral interest. They were fixed at 80% of the Hartree-Fock values.

Table 4. Fitted and Hartree-Fock energy parameters for the even Bi II configurations (cm^{-1}). Standard deviation of fit to observed levels 78 cm^{-1}.

Parameter	Fitted		HF	Fitted/HF
$6p^2$				
E_{av}	22726	±41		
F^2(pp)	29254	±376	38298	0.76
α	−63	±38		
ζ_{6p}	11808	±49	11682	1.01
6p7p				
E_{av}	101067	±32		
ζ_{6p}	13475	±40	13504	1.00
ζ_{7p}	2074	±54	1853	1.12
F^2(pp′)	7406	±338	9004	0.82
G^0(pp′)	1442	±41	2350	0.61
G^2(pp′)	1643	±288	2665	0.62
6p8p				
E_{av}	122017	±58		
ζ_{6p}	13443	±70	13575	0.99
ζ_{8p}	755		755	1.00[a]
F^2(pp′)	2676		3345	0.80[b]
G^0(pp′)	623	±41	779	0.80[b]
G^2(pp′)	765		956	0.80[b]
6p5f				
E_{av}	119341	±28		
ζ_{6p}	13633	±42	13534	1.01
ζ_{5f}	1.7		2	1.00[a]
F^2(pf)	5850	±297	6289	0.93
G^2(pf)	1469	±416	2418	0.61
G^4(pf)	1266		9961	0.80[b]
6p6f				
E_{av}	129676	±39		
ζ_{6p}	13566		13566	1.00[a]
ζ_{6f}	1.4		1	1.00[a]
F^2(pf)	2536		3170	0.80[b]
G^2(pf)	1305		1631	0.80[b]
G^4(pf)	862		1076	0.80[a]
6p7f				
E_{av}	135408[a]			
ζ_{6p}	13590		13590	1.00[a]
ζ_{7f}	0.9		0.9	1.00[a]
F^2(pf)	1454		1818	0.80[b]
G^2(pf)	835		1044	0.80[b]
G^4(pf)	554		693	0.80[a]
6p8f				
E_{av}	138866	±10		
ζ_{6p}	13605		13605	1.00[a]
ζ_{8f}	0.6		0.6	1.00[a]
F^2(pf)	908		1135	0.80[b]
G^2(pf)	551		689	0.80[b]
G^4(pf)	367		459	0.80[a]
6p7p-6p8p				
R^2(pp′, pp″)	2611	±497	4070	0.64[c]
R^0(pp′, p″p)	862	±164	1345	0.64[c]
R^2(pp′, p″p)	1013	±193	1580	0.64[c]
6p7p–6p5f				
R^2(pp′, pf)	4142	±265	4118	1.01[c]
R^2(pp′, fp)	−712	±164	−708	1.01[c]

[a] Parameter fixed at Hartree-Fock value. [b] Parameter fixed at 80% of Hartree-Fock value. [c] Ratio of CI parameters involving the same pair of configurations fixed to their HF ratio.

5.2. The odd configurations

The configurations 6p7s, 6p8s, 6p9s, 6p6d, 6p7d, 6p8d and $6s6p^3$ were included in the calculation. For the same reason as mentioned for $6p^2$, LS designations were used for $6s6p^3$. The configuration mixing is still more important for the odd configurations than for the even, as seen from the large values of the interaction parameters shown at the end of Table 5. 6p6d is strongly mixed with 6p7s, 6p7d and $6s6p^3$, and there is also a considerable mixing between 6p7d and $6s6p^3$. The configuration interaction parameters not shown in the table were fixed at 80% of the Hartree-Fock values.

In a separate ab initio calculation 6p9d and 6p10d were added to the set of configurations. As a result of this calculation the levels established at 122 278 cm^{-1} and 125 612 cm^{-1} were tentatively identified as $6p9d(1/2,3/2)_2$ and $6p10d(1/2,3/2)_2$.

6. Bi II in HR 7775

HR 7775 (= HD 193452 = β^2Cap, m_v = 6.10, B9.5 III-IVp Hg) is a slowly rotating ($v \sin i$ = 2 $km\,s^{-1}$) HgMn star. HR 7775 has previously been analysed by Adelman (1994) and Wahlgren et al. (2000) in the optical region, and by Smith & Dworetsky (1993) in the ultraviolet. The stellar parameters adopted in this work were $T_{\rm eff}$ = 10 750 K, log g = 4.0, $v \sin i$ = 2 $km\,s^{-1}$, and turbulent velocity = 0 $km\,s^{-1}$, as used by Wahlgren et al. (2000). The spectra of HR 7775 were obtained between July 2-13 1998 with the 2.56 m Nordic Optical Telescope (NOT) utilizing the SOviet-FINnish (SOFIN) echelle spectrograph (Tuominen et al. 1998; Ilyin 2000). The SOFIN spectrograph was mounted with a camera of focal length f = 1000 mm (camera 2), providing a resulting resolving power of approximately R = 80 000. In a recent investigation of HR 7775 (Wahlgren et al. 2000), it was noted that a large number of unidentified features could be found in the optical spectral region. Several of these features coincided in wavelength with Bi II lines observed in the laboratory analysis by Crawford & McLay (1934). The identification of these features as Bi II lines seemed likely since the abundance of bismuth in HR 7775, as determined from ultraviolet Bi II lines, is greatly enhanced (Jacobs & Dworetsky 1982; Wahlgren et al. 2001).

In the present investigation 14 Bi II transitions have been detected in the optical region of HR 7775. The wavelength and identification of the observed features are presented in Table 6 along with the observed intensity and a theoretical or astrophysical log gf value. Several of the Bi II features in HR 7775 are observed as either substantially broadened or as multiple spectral features, indicating the presence of noticeable hfs.

The bismuth abundance in HR 7775 and the astrophysical gf values were determined by comparing the observed spectrum to a synthetic spectrum generated with the SYNTHE (Kurucz & Avrett 1981; Kurucz 1993) program. Atomic line data were taken from the lists

Table 5. Fitted and Hartree-Fock energy parameters for the odd Bi II configurations (cm^{-1}). Standard deviation of fit to observed levels 137 cm^{-1}.

Parameter	Fitted		HF	Fitted/HF
6p7s				
E_{av}	82931	±96		
ζ_{6p}	13042	±97	13091	1.00
G^1(ps)	3855		4819	0.80[a]
6p8s				
E_{av}	115033	±115		
ζ_{6p}	13481		13481	1.00[b]
G^1(ps)	973		1216	0.80[a]
6p9s				
E_{av}	127935	±248		
ζ_{6p}	13566		13566	1.00[b]
G^1(ps)	421		526	0.80[a]
6p6d				
E_{av}	95687	±123		
ζ_{6p}	13143	±119	13015	1.00
ζ_{6d}	250		250	1.00[b]
F^2(pd)	10406	±1323	18156	0.57
G^1(pd)	11364	±380	15918	0.71
G^3(pd)	6456	±1542	9961	0.65
6p7d				
E_{av}	120129	±87		
ζ_{6p}	13521	±107	13463	1.00
ζ_{6d}	97		97	1.00[b]
F^2(pd)	4369		5461	0.80[a]
G^1(pd)	3421		4276	0.80[a]
G^3(pd)	2246		2808	0.80[a]
6p8d				
E_{av}	130338	±111		
ζ_{6p}	13558		13558	1.00[b]
ζ_{6d}	49		49	1.00[b]
F^2(pd)	1984		2480	0.80[a]
G^1(pd)	1524		1905	0.80[a]
G^3(pd)	1018		1273	0.80[a]
$6s6p^3$				
E_{av}	108290	±902		
F^2(pp)	31353	±3783	38594	0.81
α	−460	±272		
ζ_{6p}	12687	±675	11732	1.08
G^1(sp)	30585	±2046	48748	0.63
6p7s-6p6d				
R^2(ps,pd)	−11371	±1248	−12603	0.90[c]
R^1(ps,dp)	−5391	±592	−5975	0.90[c]
6p6d-6p7d				
R^2(pd,pd)	4786	±365	7210	0.66[c]
R^1(pd,dp)	5302	±408	8051	0.66[c]
R^3(pd,dp)	3399	±261	5160	0.66[c]
$6p6d-6s6p^3$				
R^1(sd,pp)	15069	±299	24725	0.61
$6p7d-6s6p^3$				
R^1(sd,pp)	9985	±676	13240	0.75

[a] Parameter fixed at 80% of Hartree-Fock value. [b] Parameter fixed at Hartree-Fock value. [c] Ratio of CI parameters involving the same pair of configurations fixed to their HF ratio.

Table 6. Observed Bi II lines in HR 7775.

λ (Å)	Int[a]	Energy levels			log gf The.[b]	log gf Ast.[c]
4079.0719	0.92	80577_1	-	105085_2		0.20
4259.4126	0.78	82257_3	-	105728_4		0.65
4272.0440	0.97	82049_2	-	105451_3		−0.40
4301.6974	0.97	82049_2	-	105289_3		0.30
4705.2854	0.96	84280_1	-	105527_2		0.20
4730.2672	0.95	88771_2	-	109905_2		0.30
4993.5338	0.98	89885_1	-	109905_2		0.30
5124.3561	0.98	88771_2	-	108280_3		0.40
5144.4921	0.89	69133_0	-	88566_1	0.01	
5209.3246	0.84	69598_1	-	88789_2	0.38	
5270.5120	0.95	69598_1	-	88566_1	−0.31	
5719.1384	0.96	69598_1	-	87078_0	−0.41	
6600.3388	0.95	69133_0	-	84280_1	−0.40	
6809.1955	0.97	69598_1	-	84280_1	−0.05	

[a] The normalized spectrum residual flux of the spectral line.
[b] Theoretical log gf values from Palmeri et al. (2001).
[c] Astrophysically determined log gf values. The error in these values is dependant on the line intensity and the two stronger and the six weaker lines are estimated to have uncertainties of ±0.2 and ±0.4 dex, respectively.

of Kurucz (1993), while the Bi II hfs components from the present laboratory analysis were individually entered into the linelists.

The determination of the bismuth abundance in stellar spectra relies heavily on the existence and quality of the atomic oscillator strengths. During the past decades both theoretical (i.e. Gruzdev 1968; Bieron et al. 1991; Palmeri et al. 2001) and experimental oscillator strengths (Osherovich & Tezikov 1978; Henderson et al. 1996) have been derived for selected Bi II lines, but there are notable discrepancies in the published data.

The determination of the bismuth abundance in the current work was made utilizing the theoretical gf values of Palmeri et al. (2001). These values were calculated using the Hartree-Fock method with relativistic corrections and the multiconfiguration Dirac-Fock fully relativistic approach. The Palmeri et al. log gf values are presented for a number of UV and visible Bi II transitions, six of which can be seen in the optical spectrum of HR 7775. It is difficult to assess the correctness of the theoretical gf values, but the close agreement between the calculated values with the experimental gf values of Henderson et al. (1996) for lines presented in both studies is an encouraging sign that the uncertainties in the calculations are small.

The bismuth abundance was determined from the two strongest Bi II lines, λ5144 and λ5209, with theoretical gf values. From these lines the abundance was determined as log N_{Bi} = 5.80 (on a scale where log N_H = 12), indicating a 5 dex enhancement over the meteoritic value log N_{Bi} = 0.71 (Grevesse & Sauval 1998). This is consistent with the results derived from Wahlgren et al. (2001). The estimated fitting error of this abundance is ±0.1 dex. This error estimate is based on synthetic spectrum fits

to the observed spectrum, and represent bismuth abundances that bracket the observed, noise-influenced, line profile. The determined abundance was then successfully utilized to obtain a fit to the four weaker Bi II features with theoretical gf values. Thus, the abundance derived from the six transitions shows good agreement, which can be interpreted as a sign of consistency in the gf value calculations of Palmeri et al.

The determination of the astrophysical log gf values in Table 6 was made utilizing the bismuth abundance determined from the Bi II features with theoretical gf values. The gf values were changed until a match was found between the synthetic and stellar spectra. Some of the Bi II features were very weak in the spectrum of HR 7775 (as indicated by their depths in Table 6), and the reality of their existence can only be substantiated by the broadness of the observed features. The weakness of most features for which astrophysical log gf values have been determined complicates the spectrum fitting and the determined log gf values are consequently quite uncertain, with an estimated uncertainty of ± 0.4 dex. The astrophysical gf values of the two strongest Bi II features in Table 6, the λ4079 and λ4259 lines, have smaller estimated uncertainties of ± 0.2 dex due to their greater line strength. The uncertainties in the log gf values represent limits in the line profile fitting as dictated by the noise level and any blending with unknown features.

The Bi II λ5209 line is the strongest bismuth feature in the optical region of HR 7775 as measured by its equivalent width. As seen from the laboratory work this line has a hfs extending over approximately 1.2 Å, and most of the individual hfs components can be seen in the stellar spectrum. In Fig. 3a the laboratory spectrum of this line is shown and compared to the spectral features in HR 7775 (Fig. 3b).

It is interesting to note that most of the strongest laboratory Bi II features are present in the spectrum of HR 7775. In fact, only three transitions, at λ4204 λ4227 and λ4391 Å, with intensities larger than 20 in Table 1 are unobserved in HR 7775. Interestingly enough, these three features originate from noticably higher energy levels than the other strong optical Bi II lines. The strength of these features in the laboratory is a reflection of the overpopulation of certain high energy levels as a result of the experimental conditions pertaining to the charge transfer within the plasma (as discussed in Sect. 2).

From Table 6 it is seen that the Bi II λ4259 and λ5209 lines are the strongest of the optical lines as measured from their normalized flux, with the latter having a significantly broader hfs than the former. These lines are therefore most useful for detecting bismuth enhancements in the optical region of CP stars. The optical features of Bi II originate from energy levels high in the term system, and a substantial bismuth enhancement is needed in order to observe these lines. Much stronger features of Bi II can, however, be found in the UV region below 2000 Å and these lines are therefore much better suited for the detection of a small to moderate abundance enhancement

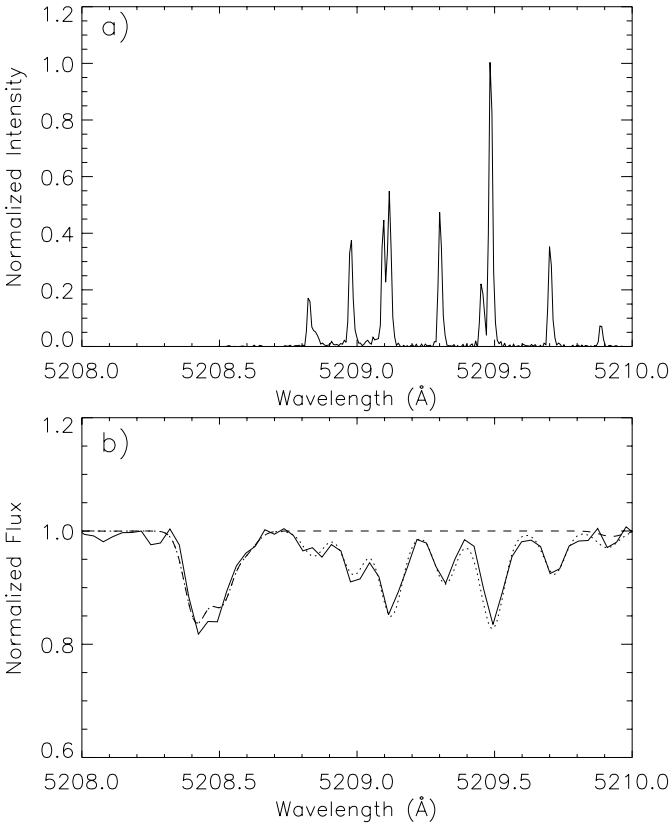

Fig. 3. The laboratory spectrum of the Bi II λ5209 line **a)** is compared to the observation of HR 7775 **b)**. For HR 7775 the observed spectrum (solid line) is compared with synthetic spectra for the solar abundance (dashed) and the best fit abundance (dotted) of bismuth.

of bismuth in the CP stars. Even though the laboratory work in the present paper only extends down to 2000 Å the wavelengths and hfs of most lines below this limit can be established since the energy levels, J values and hfs constants of almost all the energy levels below 130 000 cm^{-1} are presented in our work.

Acknowledgements. The spectra used in this work were obtained with the Nordic Optical Telescope. The Nordic Optical Telescope is operated on the island of La Palma jointly by Denmark, Finland, Iceland, Norway, and Sweden, in the Spanish Observatorio del Roque de los Muchachos of the Instituto de Astroficica de Canarias.

References

Adelman, S. J. 1994, MNRAS, 266, 97
Arcimowicz, B., & Dembczynski, J. 1979, Acta Phys. Pol. A, 56, 661
Augustyniak, L., & Werel, K. 1984, Phys. Scr., 30, 119
Bieron, J. R., Marcinek, R., & Migdalek, J. 1991, J. Phys. B, 24, 31
Bouazza, S., & Bauche, J. 1988, Z. Phys. D, 10, 1
Cole, C. D. 1964, JOSA, 54, 859
Cowan, R. D. 1981, The Theory of Atomic Structure and Spectra (University of California Press, Berkeley). The Cowan code is available at different Web sites, e.g.

http://plasma-gate.weizmann.ac.il, where a version adapted for PC by Ralchenko and Kramida can be found
Cowley, C. R. 1987, Observatory, 107, 188
Crawford, M. F., & McLay, A. B. 1934, Proc. R. Soc. London A, 143, 540
Edlén, B. 1966, Metrologia, 2, 71
Eisele, G., Koniordos, I., Müller, G., & Winkler, R. 1968, Phys. Lett., 28B, 256
Fuhrmann, K. 1989, A&AS, 77, 345
George, S., Munsee, J. H., & Verges, J. 1985, JOSA B, 2, 1258
Grabowski, D., Drozdowski, R., Kwela, J., & Heldt, J. 1996, Z. Phys. D, 38, 289
Grevesse, N., & Sauval, A. J. 1998, SSRv, 85, 161
Gruzdev, P. F. 1968, Opt. Spectrosc., 25, 1
Guthrie, B. N. G. 1972, Ap&SS, 15, 214
Guthrie, B. N. G. 1984, MNRAS, 206, 85
Henderson, M., Curtis, L. J., Ellis, D. G., Irving, R. E., & Wahlgren, G. M. 1996, ApJ, 473, 565
Ilyin, I. 2000, Ph.D. Thesis, Univ. of Oulu
Jacobs, J. M., & Dworetsky, M. M. 1982, Nature, 299, 535
Johansson, S. G., & Litzén, U. 1978, J. Phys. B, 11, L703
Karlsson, H., & Litzén, U. 2001, J. Phys. B, 34, 4475
Kurucz, R. L., & Avrett, E. H. 1981, Smithsonian Astrophys. Obs. Spec. Rep., 391
Kurucz, R. L. 1993, Synthesis Programs and Line Data, (Kurucz CD-ROM No. 18)
Leckrone, D. S., Johansson, S. G., Wahlgren, G. M., Proffitt, C. R., & Brage, T. 1998, in ASP Conf. Ser., 143, The Scientific Impact of the Goddard High Resolution Spectrograph, ed. J. C. Brandt, T. B. Ake III, & C. C. Petersen (San Fransisco: ASP), 135
Leckrone, D. S., Proffitt, C. R., Wahlgren, G. M., Johansson, S. G., & Brage, T. 1999, AJ, 117, 1454
Moore, C. E. 1958, Atomic Energy Levels, 3 (NBS Circular, no. 467)(Washington, DC:US Govt Printing Office)
Murakawa, K., & Suwa, S. 1947, Reports Inst. Sci. Tech., Tokyo Univ., 1, 121
Norlén, G. 1973, Phys. Scr., 8, 249
Osherovich, A. L., & Tezikov, V. V. 1978, Opt. Spectrosc., 44, 128
Palmeri, P., Quinet, P., & Biémont, E. 2001, Phys. Scr., 63, 468
Radziemski, L. J., Fischer, K. J., Steinhaus, D. W., et al. 1972, Comp. Phys. Commun., 3, 2
Smith, K. C., & Dworetsky, M. M. 1993, A&A, 274, 335
Stachowska, E. 1987, Ph.D. Thesis, University of Gdansk, Gdansk
Stachowska, E., Dembczynski, J., Arcimowicz, B., & Kajoch, A. 1987, Z. Phys. D, 7, 177
Tuominen, I., Ilyin, I., & Petrov, P. 1998, Astrophysics with the NOT, ed. H. Karttunen, & V. Piirola (University of Turku: Turku), 47
Wahlgren, G. M., Brage, T., Gilliland, R. L., et al. 1994, ApJ, 435, L67
Wahlgren, G. M., Dolk, L., Kalus, G., et al. 2000, ApJ, 539, 908
Wahlgren, G. M., Brage, T., Brandt, J. C., et al. 2001, ApJ, 551, 520